Bioorganic & Medicinal Chemistry 23 (2015) 192–202

Contents lists available at ScienceDirect

Bioorganic & Medicinal Chemistry

journal homepage: www.elsevier.com/locate/bmc

A dual inhibitor of matrix metalloproteinases and a disintegrin and metalloproteinases, [^{18}F]FB-ML5, as a molecular probe for non-invasive MMP/ADAM-targeted imaging

Nathalie Matusiak [a], Riccardo Castelli [b], Adriaan W. Tuin [b], Herman S. Overkleeft [b], Rosalina Wisastra [c], Frank J. Dekker [c], Laurette M. Prély [d], Rainer P. M. Bischoff [d], Aren van Waarde [a], Rudi A. J. O. Dierckx [a], Philip H. Elsinga [a,*]

[a] Department of Nuclear Medicine and Molecular Imaging, University Medical Center Groningen, University of Groningen, Hanzeplein 1, 9700 RB Groningen, The Netherlands
[b] Leiden Institute of Chemistry, Leiden University, Leiden, The Netherlands
[c] Department of Pharmaceutical Gene Modulation, Groningen Research Institute of Pharmacy, University of Groningen, Groningen, The Netherlands
[d] Department of Analytical Biochemistry, Groningen Research Institute of Pharmacy, University of Groningen, Groningen, The Netherlands

ARTICLE INFO

Article history:
Received 22 July 2014
Revised 6 November 2014
Accepted 6 November 2014
Available online 15 November 2014

Keywords:
MMPs
ADAMs
MMP/ADAM inhibitor
Hydroxamate
PET
HT1080 xenograft mouse model

ABSTRACT

Background: Numerous clinical studies have shown a correlation between increased matrix metalloproteinase (MMP)/a disintegrin and metalloproteinase (ADAM) activity and poor outcome of cancer. Various MMP inhibitors (MMPIs) have been developed for therapeutic purposes in oncology. In addition, molecular imaging of MMP/ADAM levels in vivo would allow the diagnosis of tumors. We selected the dual inhibitor of MMPs and ADAMs, ML5, which is a hydroxamate-based inhibitor with affinities for many MMPs and ADAMs. ML5 was radiolabelled with ^{18}F and the newly obtained radiolabelled inhibitor was evaluated in vitro and in vivo.

Materials and methods: ML5 was radiolabelled by direct acylation with *N*-succinimidyl-4-[^{18}F]fluorobenzoate ([^{18}F]SFB) for PET (positron emission tomography). The resulting radiotracer [^{18}F]FB-ML5 was evaluated in vitro in human bronchial epithelium 16HBE cells and breast cancer MCF-7 cells. The non-radioactive probe FB-ML5 and native ML5 were tested in a fluorogenic inhibition assay against MMP-2, -9, -12 and ADAM-17. The in vivo kinetics of [^{18}F]FB-ML5 were examined in a HT1080 tumor-bearing mouse model. Specificity of probe binding was examined by co-injection of 0 or 2.5 mg/kg ML5.

Results: ML5 and FB-ML5 showed high affinity for MMP-2, -9, -12 and ADAM-17; indeed IC_{50} values were respectively 7.4 ± 2.0, 19.5 ± 2.8, 2.0 ± 0.2 and 5.7 ± 2.2 nM and 12.5 ± 3.1, 31.5 ± 13.7, 138.0 ± 10.9 and 24.7 ± 2.8 nM. Radiochemical yield of HPLC-purified [^{18}F]FB-ML5 was 13–16% (corrected for decay). Cellular binding of [^{18}F]FB-ML5 was reduced by 36.6% and 27.5% in MCF-7 and 16HBE cells, respectively, after co-incubation with 10 μM of ML5. In microPET scans, HT1080 tumors exhibited a low and homogeneous uptake of the tracer. Tumors of mice injected with [^{18}F]FB-ML5 showed a SUV_{mean} of 0.145 ± 0.064 (n = 6) which decreased to 0.041 ± 0.027 (n = 6) after target blocking (p < 0.05). *Ex vivo* biodistribution showed a rapid excretion through the kidneys and the liver. Metabolite assays indicated that the parent tracer represented 23.2 ± 7.3% (n = 2) of total radioactivity in plasma, at 90 min post injection (p.i.).

Conclusion: The nanomolar affinity MMP/ADAM inhibitor ML5 was successfully labelled with ^{18}F. [^{18}F]FB-ML5 demonstrated rather low binding in ADAM-17 overexpressing cell lines. [^{18}F]FB-ML5 uptake showed significant reduction in the HT1080 tumor in vivo after co-injection of ML5. [^{18}F]FB-ML5 may be suitable for the visualization/quantification of diseases overexpressing simultaneously MMPs and ADAMs.

Abbreviations: ACN, acetonitrile; AcOH, acetic acid; ADAM, a disintegrin and metalloproteinase; CD, catalytic domain; DCC, *N,N′*-dicyclohexylcarbodiimide; DCM, dichloromethane; DMF, *N,N*-dimethylformamide; ECM, extracellular matrix; EOB, end of bombardment; EOS, end of synthesis; EtOAc, ethyl acetate; FBA, 4-fluorobenzoic acid; MMP, matrix metalloproteinase; MMPI, matrix metalloproteinase inhibitor; NHS, *N*-hydroxysuccinimide; PDB, Protein Data Bank; PET, positron emission tomography; p.i., post injection; PMA, phorbol 12-myristate 13-acetate; SFB, *N*-succinimidyl-4-fluorobenzoate; SPE, solid phase extraction; SPPS, solid phase peptide synthesis; TIMP, tissue inhibitor of matrix metalloproteinase; TNF, tumor necrosis factor; TSTU, *O*-(*N*-succinimidyl)-N,N,N′,N′-tetramethyluronium tetrafluoroborate; ZBG, zinc binding group.

* Corresponding author. Tel.: +31 50 3613247; fax: +31 50 3611687.
E-mail address: p.h.elsinga@umcg.nl (P.H. Elsinga).

http://dx.doi.org/10.1016/j.bmc.2014.11.013
0968-0896/

1. Introduction

The metzincins are a superfamily of multi-domain zinc(II)-dependent endopeptidases which comprise the matrix metalloproteinases (MMPs) and the a disintegrin and metalloproteinases (ADAMs).[1,2] These proteins[3] possess similar domain structure for the signal peptide, the pro-domain and the catalytic domain. In addition, the catalytic activity exhibited by the metalloproteinase domain of the ADAMs is highly homologous with the MMP catalytic domain. MMPs and ADAMs are expressed as inactive pro-proteins and require enzymatic removal of the pro-domain to become proteolytically active.[4] In addition, active MMPs and ADAMs can be inhibited by endogenous inhibitors such as tissue inhibitors of metalloproteinases (TIMPs).[5]

The diversity of biological functions implies that MMPs and ADAMs are simultaneously involved in a wide range of physiological and pathological processes.[6] To date, MMP-2 (gelatinase A, 72 kDa type IV collagenase), MMP-9 (gelatinase B, 92 kDa type IV collagenase), MMP-12 (macrophage metalloelastase) and ADAM-17 (TNF alpha converting enzyme) have attracted the most interest. MMP-2 and MMP-9 are the most extensively studied metalloproteinases because dysregulation of MMP-2 and MMP-9 is related to poor prognosis in oncology.[7–9] Many publications involving increased gelatinase expression and activity have been reported for instance in brain tumors,[10] breast cancer,[11] lung cancer,[12] skin cancer.[13] MMP-2 and MMP-9 are also upregulated in some inflammatory diseases.[14,15] MMP-12, as well as MMP-8 and MMP-14, exert anti-cancer effects. More particularly, MMP-12 is the primary protease responsible for the proteolytic liberation of angiostatin from plasminogen. Angiostatin is a protein with anti-angiogenic properties by the selective inhibition of endothelial proliferation.[16–18] Finally, ADAM-17 or TNF alpha converting enzyme (TACE) is definitely the ADAM which has attracted the most research since the discovery as the protease responsible for the release of soluble TNFα from cells.[19–21] ADAM-17 expression is upregulated in numerous tumors,[22] identically as MMP-2 and MMP-9. Besides, as TNFα is an important pro-inflammatory mediator, ADAM-17 activity has been implicated in many diseases involving inflammation such as rheumatoid arthritis,[23] Crohn's disease[24] and inflammatory bowel disorder,[25] similar as MMP-2 and MMP-9.

As both MMP and ADAM families have members which are related to some inflammatory and tumor progression processes, the ability to exploit possible synergic effects of 'cross-reactivity' of a dual inhibitor of these enzymes would be of significant interest for the characterization of inflammatory lesions or tumors.

Positron emission tomography (PET) is a molecular imaging technique which produces a detailed image of biochemical and physiological processes in living organisms by injection of a radiotracer.[26]

To achieve detection of the proteolytic activity of MMPs and ADAMs, we selected the peptidomimetic inhibitor ML5, synthesized originally by Leeuwenburgh et al.,[27,28] which is a broad-spectrum MMP/ADAM inhibitor. We radiolabelled ML5 with *N*-succinimidyl-4-[^{18}F]fluorobenzoate ([^{18}F]SFB) for PET. The binding of the obtained radiotracer [^{18}F]FB-ML5 was assessed in vitro, using human bronchial epithelium 16HBE or breast cancer MCF-7 cells. Finally, [^{18}F]FB-ML5 was tested in vivo in mice bearing HT1080 tumors.

2. Results and discussion

2.1. Design of ML5—(*R*)-N1-((*S*)-1-(((*S*)-1,6-diamino-1-oxohexan-2-yl)amino)-1-oxo-3-phenylpropan-2-yl)-N4-hydroxy-2-isobutylsuccinimide

In the design of ML5, a right hand-side inhibitor was selected. Indeed, a combined inhibitor where amino acid residues are linked on both sides of the zinc binding group (ZBG) or a left hand-side inhibitor where the amino acids are present on only the left side have shown modest inhibition.[29]

The inhibitor ML5 consists of a succinylhydroxamate attached N-terminally to a phenylalanine—lysine dipeptide (Fig. 1). The hydroxamate functions as a Zn-chelating group whereas the dipeptide part serves both as additional recognition element and as substitution handle (through the lysine residue). An isobutyl group was chosen as a P1′ substituent, a benzyl group for the P2′ substituent and a lysine for the P3′ substituent to fill, respectively, the S1′, S2′ and S3′ pocket of the active site of MMPs/ADAMs. The choice of a relatively small aliphatic substituent (isobutyl) as a P1′ residue results in a broad-spectrum affinity of ML5 for MMPs and ADAMs. The benzyl group, by its hydrophobicity, induces more affinity for MMPs and ADAMs. The need to incorporate a substituent in the third loop is still under debate considering that the S3′ pocket is an ill-defined solvent-exposed pocket. However, a lysine as a P3′ substituent can be employed for other purposes such as fluorescent labelling, biotinylation or radiolabelling through the ε-amino group.

2.2. Synthesis of ML5

The overall yield of the synthesis of the building block **9** (over 7 steps) was around 16%. The coupling by SPPS leading to ML5 (after HPLC purification) was obtained in a yield of around 5–8%.

2.3. Strategy for radiolabelling ML5

Our strategy was to radiolabel the free amine of the lysine of ML5 with the positron-emitter fluorine-18 ($T_{1/2}$ = 109.8 min) for PET. The [^{18}F]labelling of small molecules or peptides proceeds generally by conjugation of [^{18}F]prosthetic groups by [^{18}F]fluoroalkylation, [^{18}F]fluoroacylation or [^{18}F]fluoroamidation, or via click chemistry. To avoid the need of further modifications of ML5, by the incorporation of an azido or an alkyno-moiety for instance, we adopted the direct acylation in solution using *N*-succinimidyl-4-[^{18}F]fluorobenzoate ([^{18}F]SFB). [^{18}F]SFB was chosen as the [^{18}F]acylating agent because of its high in vivo stability and labelling efficiency.[30–33]

2.4. Molecular modeling of ML5 and FB-ML5

The docking of ML5 and FB-ML5 into MMP-2, MMP-9, MMP-12 and ADAM-17 are reported in the Supplementary information. According to the docking studies, the incorporation of a fluorobenzoyl substituent to the lysine moiety resulted to a moderate loss of affinity of FB-ML5 compared to the parent compound ML5 into MMP-2, MMP-9, MMP-12 and ADAM-17 (Table 1).

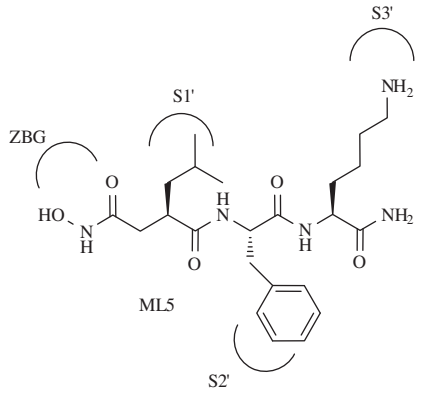

Figure 1. Structure and design of ML5.

Table 1
MolDock scores of ML5 and FB-ML5 with MMP-2, MMP-9, MMP-12 and ADAM-17

	MMP-2	MMP-9	MMP-12	ADAM-17
ML5	−133.4	−115.6	−128.0	−137.2
FB-ML5	−126.1	−118.9	−118.6	−112.9

2.5. Synthesis of the acylating agent SFB

N-Succinimidyl 4-fluorobenzoate (SFB) was prepared for further coupling with ML5 and for HPLC standard during the optimisation of the purification of [^{18}F]FB-ML5. This amide was synthesized from 4-fluorobenzoic acid (FBA) according to the literature in two different ways. In the first approach,[33] 4-fluorobenzoic acid was activated with *N*,*N*′-dicyclohexylcarbodiimide (DCC) and the resulting *O*-acylisourea was treated with *N*-hydroxysuccinimide (NHS) to give SFB. In the second method,[31] 4-fluorobenzoic acid was treated with sodium carbonate and then with *O*-(*N*-succinimidyl)-*N*,*N*,*N*′,*N*′-tetramethyluronium tetrafluoroborate (TSTU). Both methods led to SFB in good yields of 79% and 85%, respectively.

2.6. Synthesis of the reference compound FB-ML5

MMPI FB-ML5 was prepared as HPLC standard and for in vitro fluorogenic inhibition assays. FB-ML5 was prepared either by SPPS or by acylation in solution using SFB (Scheme 3). The coupling in solution using an excess of SFB led to the formation of the doubly acylated ML5: 2FB-ML5 (Fig. 2).

2.7. In vitro evaluation of ML5, FB-ML5 and 2FB-ML5 in a fluorogenic inhibition assay

The affinity of ML5, FB-ML5 and 2FB-ML5 to four selected recombinant metzincins was determined in a fluorogenic inhibition assay against MMP-2, MMP-9, MMP-12 and ADAM-17.

The IC_{50} of ML5, FB-ML5 and 2FB-ML5 against MMP-2, -9, -12 and ADAM-17 are reported in (Table 2). The incorporation of the fluorobenzoyl moiety did not result in a significant modification of the affinity for MMP-2, -9 and ADAM-17. However, FB-ML5 showed an almost 100-fold loss of affinity for MMP-12 compared to ML5. 2FB-ML5 exhibited affinity in the low micromolar range. The incorporation of a fluorobenzoyl moiety on the hydroxamic acid decreased considerably the inhibition potency of ML5.

2.8. Radiolabelling of ML5 with [^{18}F]SFB

The prosthetic group [^{18}F]SFB was prepared from 4-trimethylammonium ethylbenzoate and was synthesized in a three step procedure as described in the literature[30–33] with some modifications. The automated system produced [^{18}F]SFB with a good radiochemical yield (about 35%) with a synthesis time of about 90 min from the end of bombardment (EOB). The radiochemical purity after SPE-formulation was always more than 95%, as determined by HPLC.

The radiochemical yield of HPLC-purified [^{18}F]FB-ML5 was 13–16% based on [^{18}F]SFB (corrected for decay), the specific activity was 41–66 GBq/μmol at the end of synthesis (EOS) and the radiochemical purity >95%. The total synthesis time of [^{18}F]FB-ML5 was about 3 h (EOB).

2.9. In vitro stability of [^{18}F]FB-ML5 in human plasma and saline

After 1 h and 3 h of incubation, 99% of the radioactivity still corresponded to the intact tracer both in human plasma and saline. This indicates that [^{18}F]FB-ML5 is highly stable in vitro.

2.10. Octanol/water partition coefficient of [^{18}F]FB-ML5

The measured log*P* of [^{18}F]FB-ML5 was 1.11 ± 0.01, indicating intermediate lipophilicity.

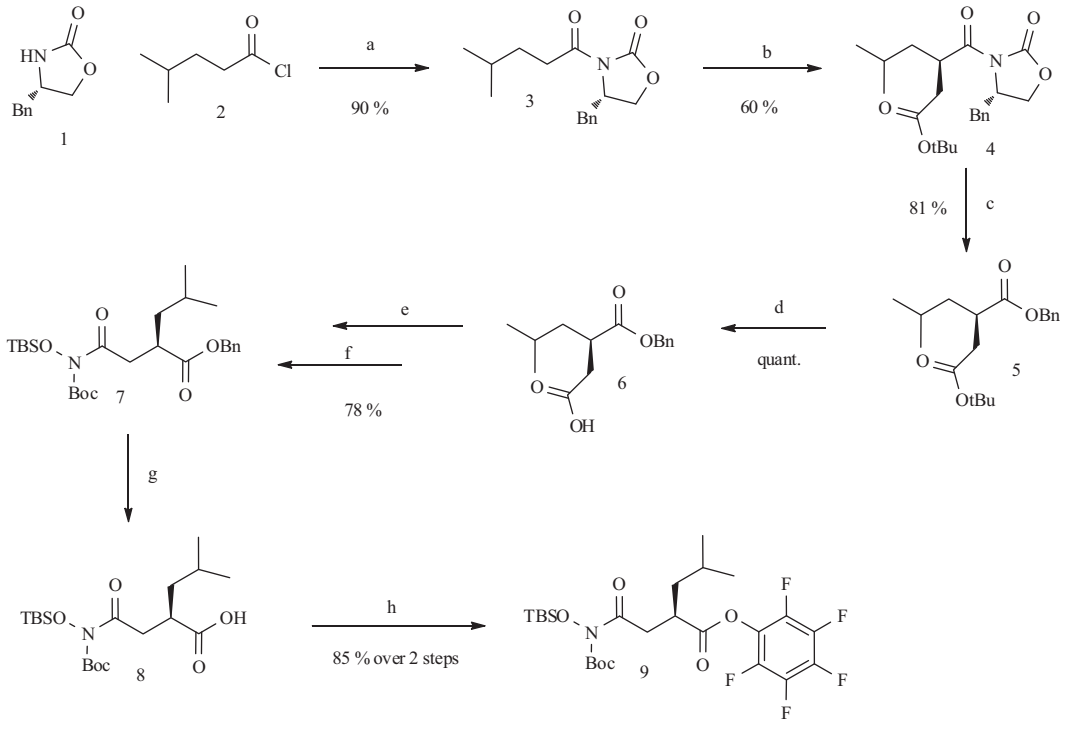

Scheme 1. Synthesis of the building block **9**. (a) 1.2 eq. n-BuLi, THF, 0 °C ; (b) 1.2 eq. LiHMDS, 1.8 eq. tBu-bromoacetate, THF, −78 °C; (c) 2 eq. BnOH, 1.2 eq. n-BuLi, THF, 0 °C; (d) TFA, DCM, RT; (e) 5 eq. $(COCl)_2$, cat. DMF, DCM, 0 °C; (f) 1.1 eq. TBSONHBoc, 2 eq. DMAP, ACN, 0 °C; (g) H_2, Pd/C, MeOH; (h) 1 eq. PFP-OH, 1 eq. EDC, DCM, RT.

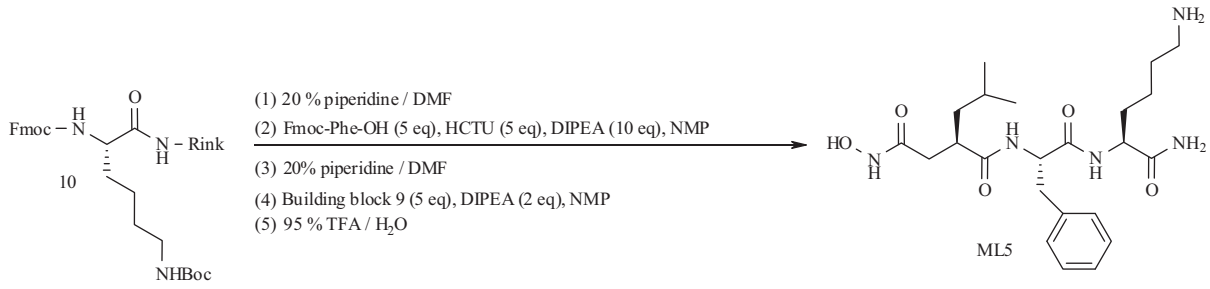

Scheme 2. Solid phase peptide synthesis towards ML5.

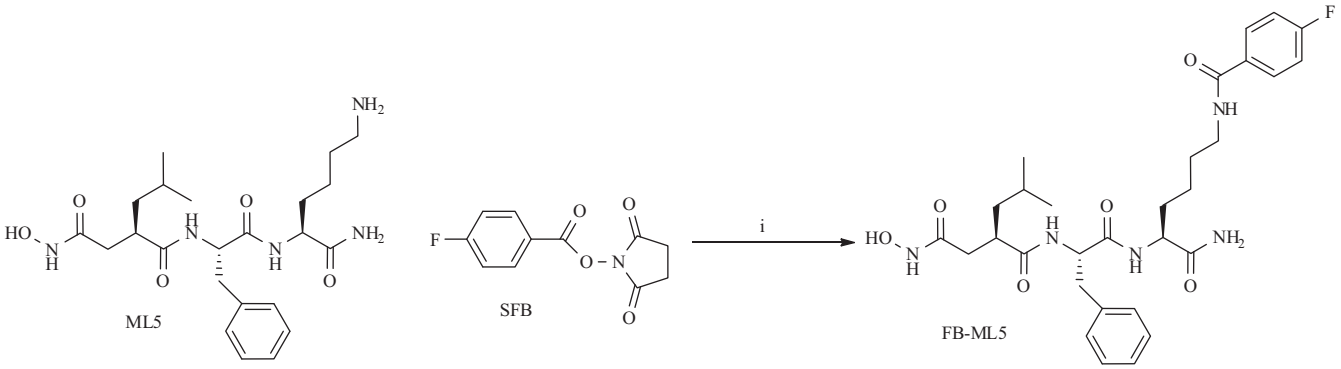

(i) ACN/phosphate buffer 0.01M pH=8.5 (1/1) (v/v), 50°C, 30 min

Scheme 3. Synthesis of FB-ML5 (with 1 equiv of SFB).

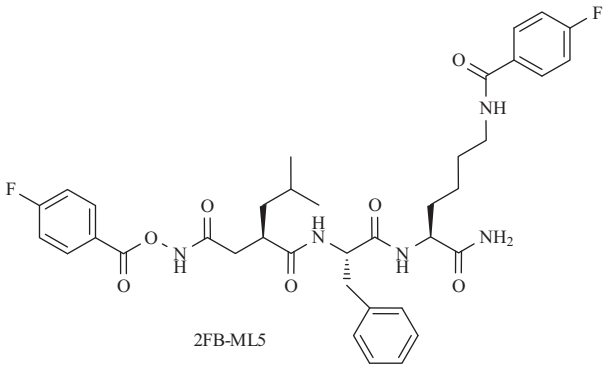

Figure 2. Structure of 2FB-ML5.

2.11. In vitro evaluation of [^{18}F]FB-ML5

Contrary to the majority of MMPs which are largely excreted proteins, ADAMs are membrane bound proteins. Therefore, the in vitro studies of [^{18}F]FB-ML5 were focused on ADAMs. We quantified the binding of the latter analogue in vitro on two human cell lines. Two cell lines, which are both overexpressing ADAM-17, were selected: the human breast cancer cell line MCF-7 and the human bronchial epithelium cell line 16HBE. MCF-7 cells were found to not express MT1-MMP (MMP-14).[34] In addition, Köhrmann et al.[35] found that MCF-7 cells express inactive MMP-14, inactive MMP-15 (MT2-MMP) but not their active forms. They also found that MCF-7 cells do not express MMP-24 (MT5-MMP). However, our aim was not to use a subtype specific cell line but to use cells as a tool to estimate overall specific binding to MMPs/ADAMs.

The association kinetics of [^{18}F]FB-ML5 was performed with MCF-7 cells by adding the radioligand at 0, 1, 2, 5, 17, 27 and 57 min (Fig. 3). At 57 min, 6.85 times more radioactivity were bound to the cells than at 0 min. The half-life of association was 7.85 min.

[^{18}F]FB-ML5 (Fig. 4) showed binding to MCF-7 cells which could be competed with non-radioactive ML5. The obtained reduction of the cellular binding was 36.6% by using 10 μM of ML5. PMA stimulation did not increase the level of binding of [^{18}F]FB-ML5 in agreement with previous work of our group.

Preliminary evaluation of [^{18}F]FB-ML5 with 16HBE cells (Fig. 5) demonstrated binding to the cells, with a binding decrease of 27.5% after blocking with 10 μM of ML5. The reduction of uptake with 10 μM of ML5 was expected to be higher, which may suggest that the non-specific binding of the tracer in 16HBE cells is apparently relatively high. As the lysine residue is solvent exposed and is not involved in the interaction with the MMP active site (Fig. 8S), the loss of affinity of [^{18}F]FB-ML5 compared to the parent compound ML5 was not anticipated. PMA and LPS stimulation did not increase the level of binding of [^{18}F]FB-ML5.

Table 2
IC_{50} values of ML5, FB-ML5 and 2FB-ML5 with MMP-2, MMP-9, MMP-12 and ADAM-17

IC_{50}	MMP-2	MMP-9	MMP-12	ADAM-17
ML5	7.4 ± 2.0 nM	19.5 ± 2.8 nM	2.0 ± 0.2 nM	5.7 ± 2.2 nM
FB-ML5	12.5 ± 3.1 nM	31.5 ± 13.7 nM	138.0 ± 10.9 nM	24.7 ± 2.8 nM
2FB-ML5	1.49 ± 0.08 μM	2.42 ± 0.40 μM	nd	3.26 ± 1.70 μM

2.12. Preclinical evaluation of [^{18}F]FB-ML5 in a HT1080 xenograft mouse model

The radiotracer [^{18}F]FB-ML5 was evaluated in a mouse model of cancer overexpressing many matrix metalloproteinases: the HT1080 xenograft mouse model. This model was already used for the evaluation of other MMP probes in fluorescent imaging notably.[36]

Plasma samples at 90 min p.i. were analysed for parent and metabolite levels by HPLC. Metabolite assays showed that the parent tracer represented 23.2 ± 7.3% (n = 2) of total radioactivity in plasma in control mice, at 90 min p.i. (Table 3). The metabolism of [^{18}F]FB-ML5 was relatively fast in plasma. According to HPLC, only more polar radio-metabolite(s) was observed (Fig. 9S). This suggests that the radiometabolite(s) is structurally different from [^{18}F]FB-ML5 and therefore probably unlikely to retain affinity for active MMPs/ADAMs.

The microPET/CT images (Fig. 6) demonstrated a homogeneous uptake throughout the tumor volume, suggesting tracer binding was not only to membrane-bound ADAMs but also to extracellular MMPs. Autoradiography of a tumor slice confirmed the regular uptake on the tumor (Fig. 10S). A high kidney uptake was also observed in the microPET/CT images.

The radioactivity uptake in the selected tissues (SUV_{mean} data presented in mean ± SD) is reported in (Fig. 7). The SUV_{mean} normalised to plasma and SUV_{mean} normalised to muscle are reported in (Figs. 8 and 9). The uptake of the radioligand in the tumor substantially ($^{**}p$ = 0.0043) decreased after co-injection of non-radioactive ML5 from a SUV_{mean} of 0.145 ± 0.064 in control mice to 0.041 ± 0.027 in block mice at 90 min p.i. The tumor to plasma ratio was 0.597 ± 0.170 versus 0.231 ± 0.171 ($^{**}p$ = 0.0039) and the tumor to muscle ratio was 3.035 ± 2.329 versus 1.084 ± 0.487 (p = 0.0724) at 90 min p.i. The change of tumor to plasma ratio was statistically significant in contrast to the change of the tumor to muscle ratio. Therefore, the binding of [^{18}F]FB-ML5 in the HT1080 xenograft mouse model was target mediated.

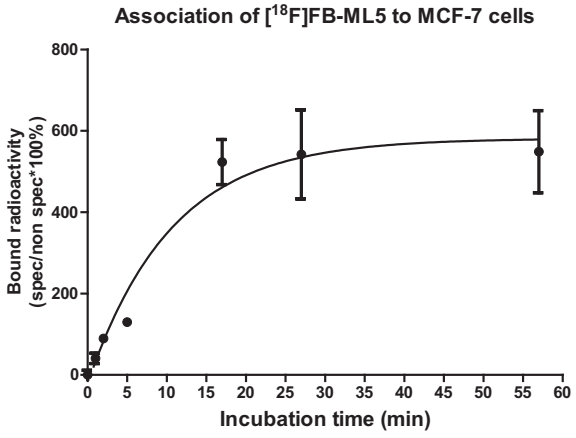

Figure 3. Time course of [^{18}F]FB-ML5 binding to MCF-7 cells.

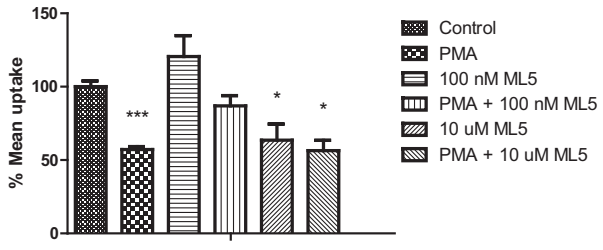

Figure 4. Specificity study of [^{18}F]FB-ML5 with MCF-7 cells.

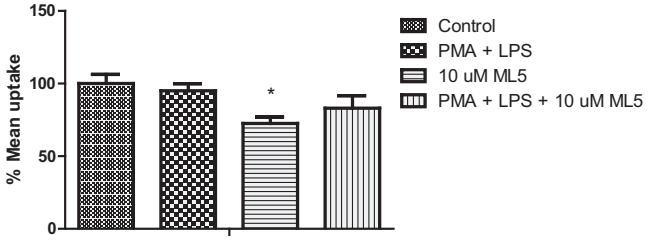

Figure 5. Specificity study of [^{18}F]FB-ML5 with 16HBE cells.

For the SUV_{mean}, the following organs were statistically different between the control and the block mice: the bone 0.041 ± 0.007 versus 0.017 ± 0.001 ($^{***}p < 0.0001$), the heart 0.111 ± 0.020 versus 0.043 ± 0.013 ($^{***}p < 0.0001$), the large intestine 1.800 ± 0.424 versus 2.750 ± 0.636 ($^{*}p$ = 0.0124), the liver 4.582 ± 0.989 versus 1.995 ± 0.148 ($^{***}p < 0.0001$), the lung 0.254 ± 0.072 versus 0.106 ± 0.045 ($^{**}p$ = 0.0016) and the plasma 0.238 ± 0.039 versus 0.185 ± 0.020 ($^{*}p$ = 0.0142).

For the tissue–plasma ratio, the bone 0.179 ± 0.060 versus 0.090 ± 0.006 ($^{**}p$ = 0.0047), the heart 0.482 ± 0.163 versus 0.235 ± 0.093 ($^{**}p$ = 0.0091), the large intestine 7.830 ± 3.069 versus 14.758 ± 1.870 ($^{***}p$ = 0.0008) and the liver 19.208 ± 1.017 versus 10.883 ± 1.959 ($^{***}p < 0.0001$) were statistically different.

Finally, for the tissue–muscle ratio, the bone 0.769 ± 0.176 versus 0.478 ± 0.136 ($^{**}p$ = 0.0094), the heart 2.069 ± 0.462 versus 1.178 ± 0.065 ($^{***}p$ = 0.0009), the large intestine 33.065 ± 5.514 versus 81.219 ± 37.415 ($^{*}p$ = 0.0109) and the lung 4.616 ± 0.546 versus 2.897 ± 0.559 ($^{***}p$ = 0.0003) were statistically different.

Table 3
Percentage of parent compound in plasma from two control mice at 90 min p.i of [^{18}F]FB-ML5

Mouse #	% of parent [^{18}F]FB-ML5
Mouse # 1	28.3
Mouse # 2	18.1

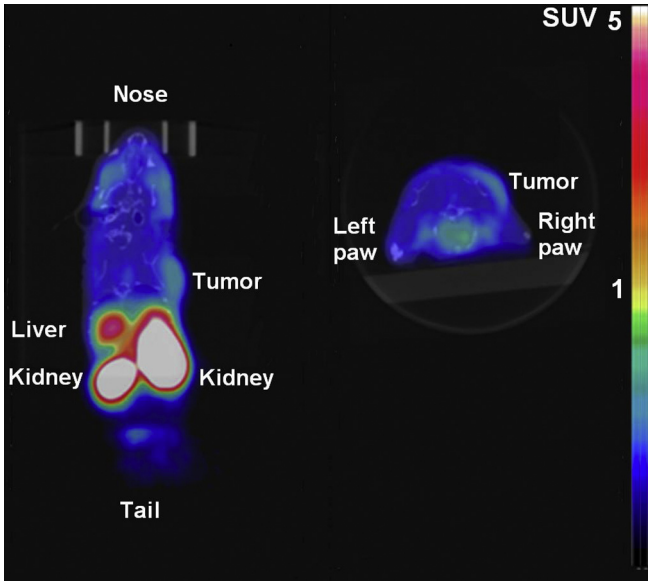

Figure 6. In vivo [^{18}F]FB-ML5 microPET/CT images of a HT1080 tumor bearing mouse shown in coronal (left) and transaxial (right) views. The microPET images correspond to the sum of all the frames from 2 to 90 min p.i. of [^{18}F]FB-ML5.

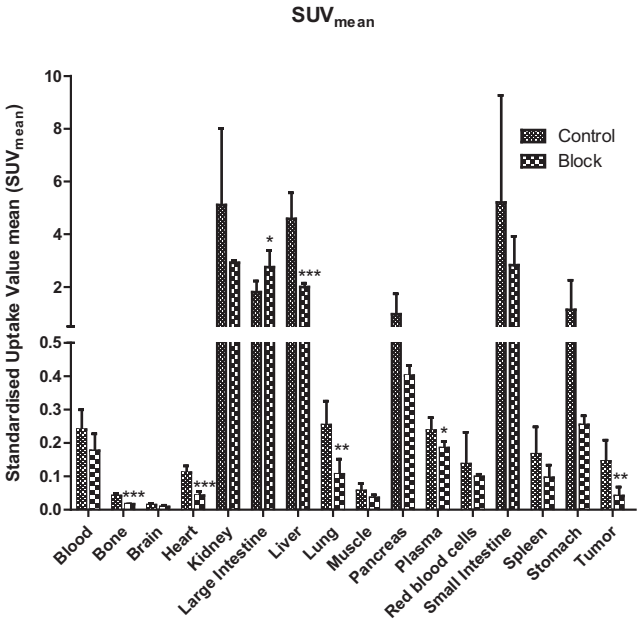

Figure 7. Ex vivo biodistribution data of tumor-bearing mice scanned with [^{18}F]FB-ML5 and tumor-bearing mice scanned with [^{18}F]FB-ML5 and co-injection of 2.5 mg/kg of ML5, at 90 min p.i. of [^{18}F]FB-ML5 ± ML5. Bars represent average and error bars SD, $n = 6$ for each group, $^{*}p < 0.05$, $^{**}p < 0.01$ and $^{***}p < 0.001$.

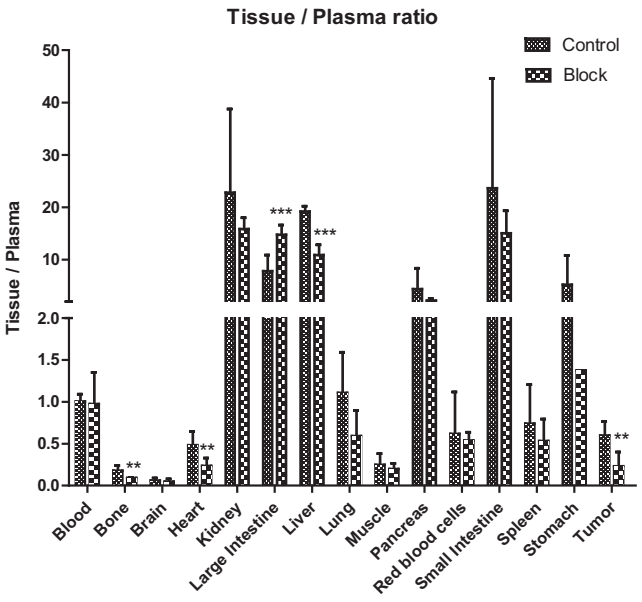

Figure 8. Tissue/plasma ratio of tumor-bearing mice scanned with [^{18}F]FB-ML5 and tumor-bearing mice scanned with [^{18}F]FB-ML5 and co-injection of 2.5 mg/kg of ML5, at 90 min p.i. of [^{18}F]FB-ML5 ± ML5. Bars represent average and error bars SD, $n = 6$ for each group, $^{**}p < 0.01$ and $^{***}p < 0.001$.

A low uptake in the bone was obtained which suggests no defluorination of the tracer. High uptakes of the radioactivity in the kidneys and to a lesser extent in the liver 90 min p.i. were obtained. This is probably due to the excretion of the radiotracer and radiometabolites. The amount of activity (i.e., tracer and metabolites) excreted by the liver into the small and large intestines was very high. Indeed, for the control mice, the SUV_{mean} obtained in the liver, small intestine and large intestine were, respectively: 4.582 ± 0.989, 5.207 ± 4.058 and 1.800 ± 0.424.

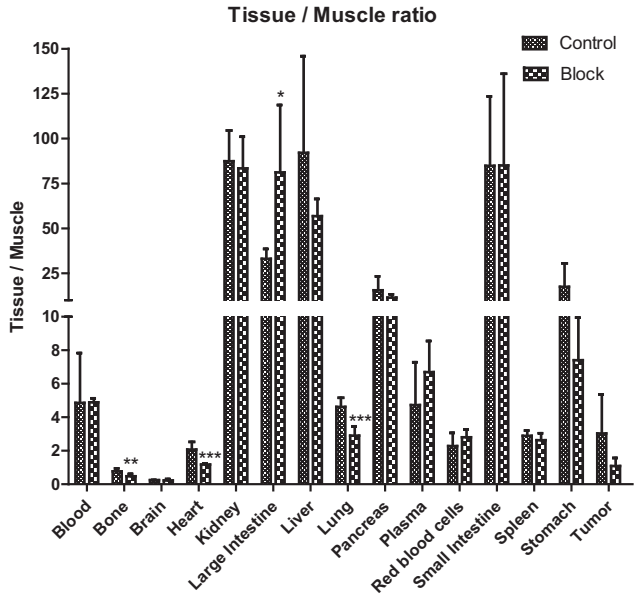

Figure 9. Tissue/muscle ratio of tumor-bearing mice scanned with [^{18}F]FB-ML5 and tumor-bearing mice scanned with [^{18}F]FB-ML5 and co-injection of 2.5 mg/kg of ML5, at 90 min p.i. of [^{18}F]FB-ML5 ± ML5. Bars represent average and error bars SD, $n = 6$ for each group, $^{*}p < 0.05$, $^{**}p < 0.01$ and $^{***}p < 0.001$.

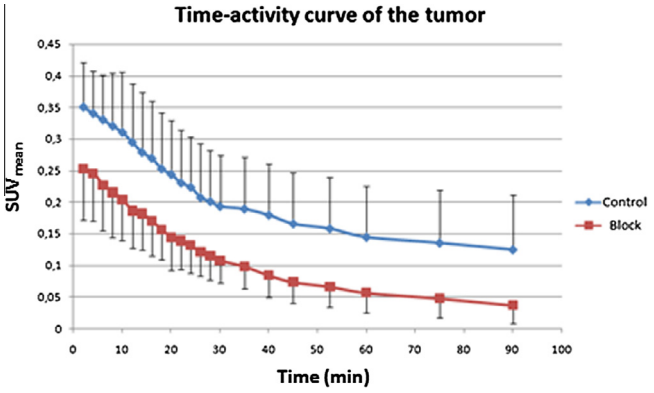

Figure 10. Time-activity curve of tumor-bearing mice scanned with [^{18}F]FB-ML5 and tumor-bearing mice scanned with [^{18}F]FB-ML5 and co-injection of 2.5 mg/kg of ML5, from 2 to 90 min p.i. of [^{18}F]FB-ML5 ± ML5. Points represent average and error bars SD, $n = 6$ for each group.

The average time-activity curves in the tumor of the control and block animals are depicted in (Fig. 10). PET-SUV_{mean} showed a significant decrease ($p = 0.0406$) of the tracer accumulation in the tumor: 0.125 ± 0.087 versus 0.037 ± 0.029 at 90 min p.i. [^{18}F]FB-ML5 demonstrated a relatively fast wash out in the tumor.

A similar MMPI based on a peptidomimetic scaffold, the radiolabelled Marimastat-ArB[^{18}F]F_3, was preliminary evaluated in a 67NR breast tumor mice.[37] A low uptake in the tumor was obtained as well and a significant reduction was obtained after pre-treatment with a non-radioactive inhibitor, which suggests that our in vivo results are quite satisfactory.

Finally, based on the multifactorial nature of numerous disease processes, the ability of a tracer to simultaneously target two pathways associated to the same disease might represent an asset in PET. As a result, the dual MMP/ADAM inhibitor [^{18}F]FB-ML5 might afford a more efficient approach to overcome the complex processes of cancer.

3. Conclusions

The MMPI ML5 was successfully radiolabelled with [^{18}F]SFB. [^{18}F]FB-ML5 showed rather low binding in MCF-7 and 16 HBE cells. [^{18}F]FB-ML5 retention showed significant reduction in the HT1080 tumor after co-injection of ML5. [^{18}F]FB-ML5 may be suitable for the visualization/quantification of pathologies overexpressing simultaneously MMPs and ADAMs.

4. Materials and methods

4.1. General

All chemicals, reagents, and solvents for the (radio)synthesis of the compounds were analytical grade, purchased from commercial suppliers (Aldrich, Fluka, Sigma and Merck) and were used without further purification, unless otherwise specified. Solid phase extraction cartridges were obtained from Waters Chromatography Division, Millipore Corporation (for SepPak Light Accell plus QMA anion exchange cartridge and SepPak C18 plus cartridge) or Merck (for LiChrolut EN cartridge and LiChrolut SCX cartridge). Flash chromatography was performed on silica gel 60 (0.040–0.063, Merck). All reactions were monitored by thin layer chromatography on Merck F-254 silica gel plates. Detection of the compounds on the TLC plates was performed with UV light (254 nm). ^{1}H, ^{13}C, and ^{19}F NMR spectra were recorded on a Varian AMX400 spectrometer (400, 100 and 200 MHz, respectively). Chemical shifts were determined relative to the signal of the solvent, converted to the TMS (tetramethylsilane) scale, and expressed in δ units (ppm) downfield from TMS (for chloroform-*d*: δ 7.261 for ^{1}H and δ 76.98 for ^{13}C, for DMSO-d_6: δ 2.504 for ^{1}H and δ 39.98 for ^{13}C and for MeOH: δ 3.312, 4.867 for ^{1}H and δ 47.84 for ^{13}C). Data are reported as follows: chemical shifts, multiplicity (s = singlet, d = doublet, t = triplet, q = quartet, dd = doublet of doublets, dt = doublet of triplets, td = triplet of doublets, m = multiplet, br = broad), coupling constants (Hz), and integration. Mass spectrometry was recorded on an AEI-MS-902 mass spectrometer by EI (70 eV) measurements. Radioactivity measurements for log*P* determination, plasma/saline stability, biodistribution and metabolites were performed using an automated gammacounter (LKB Wallac, Turku, Finland).

4.2. Statistical analysis

Calculations were performed using Excel 2007 (Microsoft) and GraphPad prism 5.0 for Windows (GraphPad Software, San Diego, USA). Results are expressed as mean ± SD. Comparisons between different experimental groups were made using unpaired two-sided student *t*-test. Data were considered statistically significant when p values were smaller than 0.05.

4.3. Molecular modeling of ML5 and FB-ML5

The crystal structures of MMPs and ADAM-17 were downloaded from the Protein Data Bank (PDB) with MMP-2 (PDB code 1HOV), MMP-9 (PDB code 2OW1), MMP-12 (PDB code 1JK3) and ADAM-17 (PDB code 2I47). All molecules were drawn using ChemaxonMarvinSketch (www.chemaxon.com) and prepared (structure recognition and protonation) using SPORES (www.tcd.uni-konstanz.de/research/spores.php). Molecular docking simulations were performed using PLANTS v1.6.140,141. The docking site center was determined by applying a constraint for the hydroxamic group to be able to form a coordination with the zinc in the active site. Fifteen poses were generated for each compound and the docking results were analyzed using Molegro Virtual Docker (www.molegro.com). Docking solutions were selected based on the MOLDOCKSCORE and the docking solutions were evaluated manually, followed by energy minimization of the ligand.

4.4. Synthesis of ML5

The peptidyl MMP inhibitor ML5 (Fig. 1) was synthesized following slight modifications of the literature procedures.[27,28] Briefly, the Evan's template **1** was prepared in a 3-step reaction from the Boc-(D)-phenylalanine. The latter analogue was treated with triethylamine and ethyl chloroformate in order to get the corresponding acid anhydride which was then reduced with sodium borohydride to give the corresponding alcohol. After treatment with thionyl chloride, the resulting *tert*-Bu-ester was transformed in its acyl chloride, which was then intramolecularly attacked by the primary alcohol to obtain the Evan's template **1**. 4-Methyl-pentanoyl chloride **2** was obtained after treatment of 4-methyl-pentanoic acid with thionyl chloride. N-Boc-O-TBS-hydroxylamine was prepared in a 2-step procedure from the hydroxylamine hydrochloride. The amino group of the latter analogue was protected with di-*tert*-butyl dicarbonate. The resulting compound was treated with *tert*-butyl dimethylsilyl chloride to give N-Boc-O-TBS-hydroxylamine. The building block **9** was prepared in 7 steps (Scheme 1), and started by deprotonation of the Evan's template **1** with *n*-butyllithium, followed by acylation with 4-methyl-pentanoyl chloride **2** to give **3**. Removal of the acidic alpha-proton with lithium bis(trimethylsilyl)amide followed by reaction of the resulting enolate with *tert*-butyl-bromoacetate gave **4**. Treatment of **4** with lithium benzyl alcoholate led to the benzyl ester **5**. The *tert*-butyl-ester **5** was then deprotected to give the intermediate **6**. The obtained carboxylic acid **6** was transformed into the corresponding acyl chloride, which was treated with N-Boc-O-TBS-hydroxylamine to give **7**. The benzyl ester in **7** was hydrolyzed by catalytic hydrogenation to the acid **8**. The carboxylic acid **8**, after activation with *N*-(3-dimethylaminopropyl)-*N*′-ethylcarbodiimide, was then acylated with pentafluorophenol to give the building block **9**. Dipeptide **10** was synthesized on Rink amide resin using standard protocols (Scheme 2). After deprotection of the Fmoc group, the Fmoc-protected phenylalanine was incorporated. Subsequent removal of the Fmoc was followed by the coupling of the building block **9** under the agency of *i*Pr$_2$EtN. The resulting compound was cleaved from the resin and simultaneously deprotected with 95% aqueous TFA. The obtained compound was purified and characterized by LCMS.

4.5. Synthesis of the acylating agent SFB

4.5.1. Synthesis of SFB by the first approach

To a solution of 4-fluorobenzoic acid (1.0 g, 7.1 mmol) and *N*-hydroxysuccinimide (0.9 g, 7.8 mmol) in 20 mL of DCM and 1 mL of DMF at 0 °C was added dropwise a solution of *N*,*N*′-dicyclohexylcarbodiimide (1.6 g, 7.8 mmol) in 10 mL of DCM at 0 °C. The reaction was stirred overnight at room temperature. The reaction was filtered to remove the *N*,*N*′-dicyclohexyl urea and the obtained filtrate was concentrated under reduced pressure. The resulting residue was partitioned between EtOAc and water. The organic layer was washed with water (3 times), brine, dried over Na_2SO_4, filtered and concentrated under reduced pressure to give the crude product. The latter was recrystallized from EtOAc–hexane to afford SFB (0.67 g) as a white solid.

4.5.2. Synthesis of SFB by the second approach

To a solution of 4-fluorobenzoic acid (0.1 g, 0.7 mmol) and sodium carbonate (0.07 g, 0.66 mmol) in 3 mL of ACN, stirred for 5 min, was added TSTU (0.21 g, 0.7 mmol). The mixture was stirred

for 1 h at 50 °C and was then filtered. The resulting filtrate was diluted with 10 mL 1% acetic acid and was passed through a Lichrolut EN cartridge. The cartridge was washed with 10 mL 0.01% AcOH/ACN (70/30) (v/v) and was dried with a stream of nitrogen. The cartridge was eluted with 3 mL of ACN and subsequent evaporation gave SFB (0.14 g) as a white product.

^{1}H NMR (chloroform-*d*) δ 8.24–8.13 (m, 2H), 7.48–7.37 (m, 2H), 2.81 (s, 4H).

4.6. Synthesis of the reference compound FB-ML5

4.6.1. Synthesis of FB-ML5 by SPPS

The SPPS resulting to the reference compound FB-ML5 followed a procedure identical to the synthesis of ML5.

4.6.2. Synthesis of FB-ML5 in solution

The acylation in solution with NHS-coupling agents proceeds generally in borate buffer at pH 8.5. However, it was shown that boronic acid complex can be formed with hydroxamic acid moieties.[38] As ML5 contains a hydroxamic acid, we considered phosphate buffer as a substitute of borate buffer. This buffer was prepared by a $Na_2HPO_4{\cdot}12H_2O$ 1 M/$NaH_2PO_4{\cdot}H_2O$ 1 M (93.2/6.8) (v/v) solution and by adjustment of the pH to 8.5 with sodium hydroxide 1 M. ML5 (0.50 mg, 1.08 μmol, 500 μL) dissolved in phosphate buffer pH 8.5 (0.01 M) was transferred to SFB (1.08 μmol, 500 μL) in ACN. The reaction mixture was allowed to react for 30 min at 50 °C. The reaction was quenched with HCl (1 mL, 0.25 M). Then an aliquot of 100 μL was injected through an analytical HPLC, using a Phenomenex Luna C18 column (4.6 mm × 250 mm, 5 μm) from Waters, preceded of a 20 × 4.6 mm^2 precolumn. Gradient elution was performed using a mixture of H_2O + 0.1% TFA (solvent A) and CH_3CN + 0.1% TFA (solvent B). A linear gradient (overall time = 60 min) starting from 95% solvent A in solvent B to 100% solvent B at 60 min was employed at a flow rate of 1 mL min^{-1}. The column effluent was monitored using an Elite Lachrom VWR Hitachi L-2400 UV detector (λ = 254 nm, AUFS = 0.010) and a Bicron frisk-tech radioactivity detector. Sample injection was carried out using an injector block with a loop of 100 μL. Fractions of 1 min were collected and the formed products were identified by mass spectrometry.

The retention time of FB-ML5 was 37 min.

ESI-MS (*m*/*z*): 586.5 [M+H]+, calcd 586.7; 608.5 [M+Na]+, calcd 608.7.

4.6.3. Synthesis of FB-ML5 in solution by using an excess of acylating agent

ML5 (0.50 mg, 1.08 μmol, 500 μL) dissolved in phosphate buffer pH 8.5 (0.01 M) was transferred to SFB (5.40 μmol, 500 μL) in ACN. The reaction mixture was allowed to react for 30 min at 50 °C. The reaction was quenched with HCl (1 mL, 0.25 M). Then an aliquot of 100 μL was injected through an analytical HPLC, as previously described. Fractions of 1 min were collected and the formed products were identified by mass spectrometry.

The obtained product was 2FB-ML5 with a retention time of 25.7 min.

ESI-MS (*m*/*z*): 708.4 [M+H]+, calcd 708.8; 730.4 [M+Na]+, calcd 730.8.

4.7. In vitro evaluation of ML5, FB-ML5 and 2FB-ML5 in a fluorogenic inhibition assay

Recombinant ADAM-17 (ectodomain) was purchased from R&D Systems (Minneapolis, MN, USA). Recombinant catalytic domain (CD) of human MMP-2 was from Biomol International (Butler Pike, PA, USA). Recombinant human MMP-12 CD and recombinant human MMP-9 CD without fibronectin type II insert (expressed in *Escherichia coli* as described in Refs. 39,40) were a kind gift from AstraZeneca R&D (Lund & Moelndal, Sweden).

This competitive enzyme activity assay was performed by monitoring the conversion of the fluorogenic substrate Mca-PLAQAV-Dpa-RSSSR-NH_2 (R&D systems) by recombinant ADAM-17 in the presence of increasing concentrations of ML5, FB-ML5 or 2FB-ML5. For MMP-2, -9 and -12, the conversion of the fluorogenic substrate Mca-Pro-Leu-Gly-Leu-Dpa-Ala-Arg-NH_2 (Bachem, Bubendorf, Switzerland) was followed. Measurements were performed in Costar White 96-well plates (Corning, Schiphol-Rijk, The Netherlands), where each well contained 10 ng ADAM-17 and a final concentration of 10 μM substrate in a final volume of 100 μL ADAM assay buffer (25 mM Tris pH 9.0, 2.5 μM $ZnCl_2$, 0.005% w/v Brij-35). Inhibition of MMP proteolytic activity was determined with 10 ng of MMP-2, MMP-9 or MMP-12 per well with a final concentration of 2 μM substrate in 100 μL MMP assay buffer (50 mM Tris pH 7.4, 0.2 M NaCl, 10 mM $CaCl_2$, 2.5 μM $ZnCl_2$, 0.05% v/v Brij-35). Proteolysis rates were followed by measuring fluorescence ($\lambda_{ex,em}$ = 320, 440 nm) increase using a Fluostar Optima plate reader (BMG Labtech, Offenburg, Germany), at 20 °C for recombinant MMPs and at 37 °C for recombinant ADAM-17, for 15 min (conditions of the experiments not in the stationary phase). For ML5, eleven-point inhibition curves (0, 0.5, 1, 2, 6, 12, 25, 50, 100, 500 and 1000 nM) were plotted in GraphPadPrism 5.0 for Windows (GraphPad Software, San Diego, USA). For FB-ML5, nine-point inhibition curves (0, 5, 10, 20, 60, 125, 250, 500 and 1000 nM) were plotted. For 2FB-ML5, six-point inhibition curves (0, 0.1, 1, 5, 10 and 100 μM) were plotted. IC_{50} values were determined by sigmoidal fitting. Each experiment was performed in triplicate.

4.8. Synthesis of 4-trimethylammonium ethylbenzoate triflate

To a solution of ethyl-4-dimethylaminobenzoate (0.65 g, 3.36 mmol) dissolved in 12 mL of anhydrous benzene was added dropwise methyltrifluoromethanesulfonate (0.42 mL, 3.70 mmol). The mixture was heated to reflux for 6 h and was then stirred overnight at room temperature. The reaction mixture was concentrated under reduced pressure and the resulting crude precipitate was recrystallized with diethyl ether to yield 1.01 g (84%) of white product.

^{1}H NMR (chloroform-*d*) δ 8.06–7.97 (m, 2H), 7.78–7.71 (m, 2H), 4.31 (q, *J* = 6.0 Hz, 2H), 3.70 (s, 9H), 1.32 (t, *J* = 5.8 Hz, 3H).

4.9. Radiosynthesis of no-carrier-added *N*-succinimidyl-4-[^{18}F]fluorobenzoate ([^{18}F]SFB)

Aqueous [^{18}F]fluorine was produced by irradiation of [^{18}O]-water with a Scanditronix MC-17 cyclotron via the ^{18}O(p,n) ^{18}F nuclear reaction. The [^{18}F]fluorine solution was passed through a SepPak Light Accell plus QMA anion exchange cartridge (preconditioned with 5 mL of sodium bicarbonate 1.4% and 100 mL of H_2O and then dried under a flow of Argon) to recover the [^{18}O]-enriched water. The [^{18}F]fluorine was eluted from the QMA anion exchange cartridge with 1 mg potassium carbonate in 1 mL of water and collected into a vial containing 5 mg kryptofix[2.2.2]. Subsequently, 1 mL of anhydrous acetonitrile was added and the solvents were removed at 130 °C under an argon stream. The [^{18}F]KF/kryptofix[2.2.2] complex was then dried by azeotropic distillation with 3 times addition of 0.5 mL anhydrous acetonitrile at 130 °C. A solution of 10 mg 4-trimethylammonium ethylbenzoate triflate in 250 μL anhydrous DMF was added to the [^{18}F]KF/kryptofix[2.2.2] complex. The radiofluorination was performed at 90 °C for 12 min. Thereafter, 0.5 mL of 1 M HCl was added and the hydrolysis of 4-[^{18}F]fluoroethylbenzoate was performed for 5 min at 100 °C. After cooling, crude 4-[^{18}F]fluorobenzoic acid ([^{18}F]FBA)

was passed through a SepPak C18 plus cartridge (preconditioned with 10 mL of EtOH and 10 mL of H_2O). The reaction vial was rinsed with 2 mL H_2O which were passed through the SepPak C18 plus cartridge. To remove unreacted 4-trimethylammonium ethylbenzoate, a cation exchange extraction SCX cartridge (preconditioned with 3 mL of HCl 0.1 M and 100 mL of H_2O and then dried under a flow of Argon) was connected to the SepPak C18 plus cartridge. Purified [^{18}F]FBA was eluted from the SepPak C18 plus/SCX cartridges with 2 mL acetonitrile in a vial containing 10 mg kryptofix[2.2.2], 5 mg K_2CO_3 and 50 μL H_2O. As [^{18}F]FBA is highly volatile, it was converted to [^{18}F]fluorobenzoate which was coevaporated 3 times with 0.5 mL acetonitrile in the presence of kryptofix[2.2.2] and potassium carbonate. The resulting salt was treated with freshly dissolved *O*-(*N*-succinimidyl)-N,N,N',N'-tetramethyluronium tetrafluoroborate (TSTU) in 0.5 mL acetonitrile for 5 min at 90 °C to allow the formation of [^{18}F]SFB. After cooling, the production of [^{18}F]SFB was completed by addition of 1 mL HCl 0.03 M.

4.10. Purification of *N*-succinimidyl-4-[^{18}F]fluorobenzoate by SPE

[^{18}F]SFB was diluted with 15 mL of water for injection and passed through an Oasis HLB 30 mg (1 cc) cartridge for solid phase extraction. The cartridge was washed with 10 mL of water and eluted with 500 μL acetonitrile to give the purified [^{18}F]SFB.

4.11. Radiosynthesis of [^{18}F]FB-ML5

[^{18}F]SFB dissolved in 500 μL acetonitrile was added to a solution of ML5 (0.50 mg, 1.08 μmol) in 500 μL 0.01 M phosphate buffer pH 8.5. The reaction was performed at 50 °C for 30 min. After cooling, the reaction mixture was diluted with 600 μL acetonitrile and 600 μL H_2O and was purified by semi-preparative reverse phase HPLC. HPLC was performed with Elite LaChrom Merck Hitachi L-7100 pump system using a Phenomenex reversed-phase Luna C18 column (10 mm × 250 mm, 5 μm), preceded of a 20 × 4.6 mm^2 precolumn, equipped with both UV (Elite LaChrom VWR Hitachi L-2400 UV detector set at 254 nm, AUFS = 0.5) and a Bicron radioactivity monitor. Sample injection was carried out using an injector block with a loop of 1 mL. Gradient elution was performed using a mixture of 0.01 M monosodium phosphate buffer (NaH_2PO_4) pH 6.0 (solvent A) and ACN (solvent B). The following gradient profile (overall time = 47 min) at a flow rate of 2.5 mL min^{-1} was used: 30% of ACN in solvent A over 5 min, followed by a linear gradient from 30% to 60% of ACN in solvent A over 40 min and followed by a linear gradient from 60% to 10% of ACN in solvent A over 2 min. The retention time of [^{18}F]FB-ML5 was about 20.3 min (18.1–22.6 min). The HPLC-collected fraction was diluted with about 100 mL of water for injection and passed through an Oasis HLB 30 mg (1 cc) cartridge. The cartridge was washed with 10 mL of water for injection and eluted with 0.7 mL of EtOH. The obtained product was redissolved in saline to decrease the percentage of EtOH to less than 10% for the subsequent cell/animal experiments.

Quality control was performed as described for FB-ML5. The retention time of [^{18}F]FB-ML5 was 37 min.

4.12. In vitro stability of [^{18}F]FB-ML5 in human plasma and saline

4.12.1. Human plasma stability

The stability of [^{18}F]FB-ML5 was evaluated in vitro in human plasma. Whole blood from a healthy donor, kept at room temperature for 15 min, was centrifuged at 3000 rpm for 5 min, subsequently the supernatant was taken. 100 μL of formulated [^{18}F]FB-ML5 was dissolved in 1 mL human plasma and incubated at 37 °C for 3 h. After 1 h and 3 h of incubation, aliquots of 250 μL were taken. 750 μL of ACN were added in order to deproteinize the plasma, and the mixture was centrifuged for 3 min at 3000 rpm. The supernatant was passed through a Millex Filter (0.22 μm), diluted with 600 μL ACN and 600 μL H_2O and analysed by semi-preparative HPLC using a Phenomenex reversed-phase Luna C18 column (10 mm × 250 mm, 5 μm), preceded by a 20 × 4.6 mm^2 precolumn. Gradient elution was performed using a mixture of 0.01 M monosodium phosphate buffer (NaH_2PO_4) pH 6.0 (solvent A) and ACN (solvent B). The following gradient profile (overall time = 47 min) at a flow rate of 2.5 mL min^{-1} was used: 30% of ACN in solvent A over 5 min, followed by a linear gradient from 30% to 60% of ACN in solvent A over 40 min and followed by a linear gradient from 60% to 10% of ACN in solvent A over 2 min. Fractions of the eluate were collected every minute and radioactivity in the fractions was determined with a gammacounter (LKB Wallac, Turku, Finland).

4.12.2. Saline stability

The stability of [^{18}F]FB-ML5 was evaluated in vitro in saline. Formulated [^{18}F]FB-ML5 was dissolved in 1 mL saline and incubated at 37 °C for 3 h. After 1 h and 3 h of incubation, aliquots of 250 μL were taken and diluted with 1 mL ACN and 1 ml H_2O and analysed by semi-preparative HPLC as described above. Fractions of the eluate were collected every minute and radioactivity in the fractions was determined with a gammacounter (LKB Wallac, Turku, Finland).

4.13. Octanol/water partition coefficient of [^{18}F]FB-ML5

About 5 kBq of formulated [^{18}F]FB-ML5 diluted in 5 μL saline was diluted in 495 μL PBS (pH = 7.4) and 500 μL *n*-octanol in an Eppendorf cup. The mixture was vortexed for 5 min and the cup was centrifuged at 3000 rpm for 5 min. Radioactivity in 100 μL aliquots of the water and *n*-octanol layers was determined in a gammacounter (LKB Wallac, Turku, Finland). The experiment was performed in triplicate. The partition coefficient ($\log P$) was calculated as:

$$\log P = \log_{10}\left(\frac{\text{cpm}_{\text{octanol layer}}}{\text{cpm}_{\text{aqueous layer}}}\right)$$

4.14. In vitro evaluation of [^{18}F]FB-ML5

Human breast cancer MCF-7 cells and human bronchial epithelium 16HBE cells were obtained from American Type Culture Collection, Manassas, USA. MCF-7 and 16HBE cells were maintained in 15 mL Eagle's Minimum Essential Medium (EMEM) (Lonza, Walkersville, USA) supplemented with 10% fetal calf serum (FCS) in a T_{75} culture flask. Cells were grown in a humidified atmosphere containing 5% CO_2 and were passaged twice per week.

For 16HBE cells: 16HBE cells were seeded in a 24-well plate at 50.000 cells/mL 6 days before the experiment. An equal number of cells were dispensed in each well in 0.5 mL of serum-containing medium: EMEM supplemented with 10% FCS. Cells were grown to confluency and serum-starved overnight. One day before the experiment, the medium was changed to low serum medium: EMEM supplemented with 0.5% FCS.

For MCF-7 cells: MCF-7 cells were seeded in a 12-well plate 48 h before the experiment. An equal number of cells were dispensed in each well in 1 mL of serum-containing medium: EMEM supplemented with 10% FCS. Cells were grown to confluency and serum-starved overnight. One day before the experiment, the

medium was changed to low serum medium: EMEM supplemented with 0.5% FCS.

Binding/specificity studies were performed when confluency had reached 80–90%.

For binding study with MCF-7 cells: 0.5 MBq of [^{18}F]FB-ML5 in <50 μL of saline (containing maximum 10% of absolute ethanol) were added to each well. After 57 min of incubation, the medium was quickly removed and the monolayer was washed 3 times with PBS. Cells were then treated with 0.2 mL of trypsin. When the monolayer had detached from the bottom of the well, 0.8 mL of EMEM supplemented with 10% FCS was added to stop the proteolytic action. Cell aggregates were resolved by repeated pipetting of the trypsin/EMEM mixture. Radioactivity in the cell suspension (1 mL) was assessed using a gamma counter for 15 s. A sample of the suspension was mixed with trypan blue solution (1:1 v/v) and was used for cell counting. Cell numbers were determined manually, using a phase contrast microscope (Olympus, Tokyo, Japan), a Bürker bright-line chamber (depth 0.1 mm; 0.0025 mm^2 squares) and a hand tally counter. All experiments were performed as a quadruplicate study with at least two repeats.

4.14.1. For specificity study

For 16HBE cells: four different experimental conditions were examined in quadruplicate: non-stimulated cells, non-stimulated cells + 10 μM of non-radioactive ML5 (10 μL), stimulated cells (25 ng/mL PMA and 100 ng/mL LPS added 60 min before [^{18}F]FB-ML5 addition) and stimulated cells + 10 μM of ML5 (10 μL). Blocker was added 2 min before tracer addition. 0.5 MBq of [^{18}F]FB-ML5 in <50 μL of saline (containing maximum 10% of absolute ethanol) was added to each well and incubated for 60 min. After washing 3 times with 500 μL PBS, the cells were detached with 100 μL of trypsin and transferred to test tubes. After addition of 400 μL of EMEM + 10% FCS and resuspension, radioactivity in the cell suspension (0.5 mL) was assessed using a gamma counter. A sample of the suspension was mixed with trypan blue solution (1:1 v/v) and was used for cell counting. Cell numbers were determined manually, using a phase contrast microscope, a Bürker bright-line chamber and a hand tally counter.

For MCF-7 cells: six different experimental conditions were examined in quadruplicate: non-stimulated cells, non-stimulated cells + 100 nM of ML5 (10 μL), non-stimulated cells + 10 μM of ML5 (10 μL), stimulated cells (100 nM PMA added 2.5 h before [^{18}F]FB-ML5 addition), stimulated cells + 100 nM of ML5 (10 μL) and stimulated cells + 10 μM of ML5 (10 μL). Blocker was added 2 min before tracer addition. 0.5 MBq of [^{18}F]FB-ML5 in <50 μL of saline (containing maximum 10% of absolute ethanol) was added to each well and incubated for 60 min. After washing 3 times with 1 mL PBS, the cells were detached with 200 μL of trypsin and transferred to test tubes after addition of 800 μL of EMEM + 10% FCS and resuspension. Radioactivity in the cell suspension (1 mL) was assessed using a gamma counter. A sample of the suspension was mixed with trypan blue solution (1:1 v/v) and was used for cell counting. Cell numbers were determined manually, using a phase contrast microscope, a Bürker bright-line chamber and a hand tally counter.

4.15. HT1080 fibrosarcoma xenograft mouse model

4.15.1. Animals

Male BALB/c nu/nu (BALB/cOlaHsd-Foxn1nu) mice (nude mice) were obtained from Harlan (Lelystad, The Netherlands). The mice were housed in IVC cages with paper bedding on a layer of wood shavings in a room with constant temperature (~20 °C) and fixed, 12-h light–dark regime. Food (standard laboratory chow, RMH-B, Hope Farms, The Netherlands) and water were available ad libitum. After arrival, the mice were allowed to acclimatize for at least seven days. The study was approved by the Animal Ethics Committee of the University of Groningen, The Netherlands (DEC 6058B).

4.15.2. HT1080 inoculation

Human fibrosarcoma HT1080 cells were obtained from American Type Culture Collection, Manassas, USA. HT1080 cells were maintained in 15 mL EMEM supplemented with 10% FCS in a T_{75} culture flask. Cells were grown in a humidified atmosphere containing 5% CO_2 and were passaged twice per week. $(2–2.5) \times 10^6$ HT1080 cells, in a 1:1 (v/v) mixture of Matrigel (extracellular matrix compound, Becton Dickinson) and EMEM with 10% FCS, were subcutaneously injected into the right shoulder of the BALB/c nude mice (7–8 weeks old).

4.16. MicroPET studies

Animals were scanned when the tumors reached an adequate size (0.3–0.6 mL), 14 to 21 days after inoculation. The mice were randomly divided into two groups: tumor-bearing mice scanned with [^{18}F]FB-ML5 and tumor-bearing mice scanned with [^{18}F]FB-ML5 and coinjection of 2.5 mg/kg of ML5. [^{18}F]FB-ML5 (6.1 ± 2.3 MBq, 0.15 ± 0.09 nmol), dissolved in saline, was intravenously injected into the penile vein of mice anesthetized with 5% isoflurane (Pharmacie BV, The Netherlands) in medical air at a flow rate of 2 mL min^{-1}, after which anesthesia was maintained with 2% isoflurane. Following induction of anesthesia, the mice were positioned on the bed of the microPET camera (Focus 220, Siemens Medical Solutions USA, Inc.) in transaxial position. The body temperature of the mice was maintained by electronically regulated heating pads. Data acquisition of the microPET camera was initiated and continued for a period of 90 min. After completion of the dynamic emission scan, a 515 s transmission scan with a Co-57 point source was performed for correction of attenuation of 511 keV photons by tissue. After microPET scanning, the mice were terminated by administering a high dose of isoflurane (5%) for about 20 min.

4.17. MicroCT

After the microPET scan, a computed tomography (CT) scan was performed for attenuation correction and to provide anatomical localization. The sacrificed mouse attached to the bed was inserted to the microCT scanner (MicroCAT II, CTI Siemens) and a microCT image (exposure time = 1050 ms; X-ray voltage = 55 kvp; anode current = 500 μA; number of rotation steps = 500; total rotation = 360°) was acquired for 15 min.

4.18. Ex vivo biodistribution

After the microPET scan, the ex vivo biodistribution was performed on the sacrificed mice. The following organs were taken: bladder, bone, brain, heart, kidney, large intestine, liver, lungs, muscle, pancreas, small intestine, spleen, stomach, tumor and urine. A small drop of infusate was taken for data correction. The blood was centrifuged in order to collect plasma and red blood cells. All the organs and infusate were weighed and analyzed for the amount of radioactivity, using a gammacounter (LKB Wallac, Turku, Finland). Tracer uptake was expressed as the standardized uptake value (SUV_{mean}), defined as [tissue activity concentration (MBq/g)/(injected activity (MBq)/mouse body weight (g))]. The tumor-to-plasma and tumor-to-muscle ratios were also determined.

4.19. MicroPET image analysis

Emission sinograms were iteratively reconstructed (OSEM2d) after being normalized, corrected for attenuation, scatter and

decay of radioactivity. The list-mode data of the emission scans were separated into 22 frame sinograms (15 frames of 2 min, 3 frames of 5 min, 2 frames of 7.5 min, 2 frames of 15 min). PET image analysis was performed using Inveon Research Workplace (Siemens) software. Regions of interest were drawn around the tumor. Tracer uptake in the region of interest was determined as Bq cm^{-3} and converted to PET-SUV_{mean} using the following formula: [tissue activity concentration (MBq/cc)/(injected activity (MBq)/mouse body weight (g))].

4.20. Metabolite analysis (plasma) of [^{18}F]FB-ML5 in a HT1080 xenograft mouse model

Metabolite analysis was performed on plasma collected after the ex vivo biodistribution study. 750 μL of ACN was added to 250 μL of plasma, the mixture was then centrifuged for 3 min at 3000 rpm. The supernatant was passed through a Millex Filter (0.22 μm), diluted with 600 μL acetonitrile and 600 μL H_2O, and analysed by semi-preparative HPLC. Fractions of the eluate were collected every minute and radioactivity in these fractions was then determined with a gammacounter (LKB Wallac, Turku, Finland).

Acknowledgements

The authors wish to thank the Dutch Technology Foundation (STW) for financial support (project 08008).

Supplementary data

Supplementary data associated with this article can be found, in the online version, at http://dx.doi.org/10.1016/j.bmc.2014.11.013.

References and notes

1. Seals, D. F.; Courtneidge, S. A. *Genes Dev.* **2003**, *17*, 7.
2. Nagase, H.; Woessner, J. F. *J. Biol. Chem.* **1999**, *274*, 21491.
3. White, J. M. *Curr. Opin. Cell Biol.* **2003**, *15*, 598.
4. MacFadyen, R. J. *Curr. Opin. Pharmacol.* **2007**, *7*, 171.
5. Hu, J.; Van den Steen, P. E.; Sang, Q.-X. A.; Opdenakker, G. *Nat. Rev. Drug Disc.* **2007**, *6*, 480.
6. Hidalgo, M.; Eckhardt, S. G. *J. Natl. Cancer Inst.* **2001**, *93*, 178.
7. Wiley, J. P.; Hughes, K. A.; Kaiser, R. J.; Kesicki, E. A.; Lund, K. P.; Stolowitz, M. L. *Bioconjugate Chem.* **2001**, *12*, 240.
8. Konstantinopoulos, P. A.; Karamouzis, M. V.; Papatsoris, A. G.; Papavassiliou, A. G. *Int. J. Biochem. Cell Biol.* **2008**, *40*, 1156.
9. Björklund, M.; Koivunen, E. *Biochim. Biophys. Acta* **2005**, *1755*, 37.
10. Klein, G.; Vellenga, E.; Fraaije, M. W.; Kamps, W. A.; de Bont, E. S. J. M. *Crit. Rev. Oncol. Hematol.* **2004**, *50*, 87.
11. Forsyth, P. A.; Wong, H.; Laing, T. D.; Rewcastle, N. B.; Morris, D. G.; Muzik, H.; Leco, K. J.; Johnston, R. N. *Br. J. Cancer* **1999**, *79*, 1828.
12. Somiari, S. B.; Somiari, R. I.; Heckman, C. M.; Olsen, C. H.; Jordan, R. M.; Russell, S. J.; Shriver, C. D. *Int. J. Cancer* **2006**, *119*, 1403.
13. Nawrocki, B.; Polette, M.; Marchand, V.; Monteau, M.; Gillery, P.; Tournier, J.-M. *Int. J. Cancer* **1997**, *72*, 556.
14. Zhou, M.; Qin, S.; Chu, Y.; Wang, F.; Chen, L.; Lu, Y. *Int. J. Clin. Exp. Pathol.* **2014**, *7*, 3048.
15. Meijer, M. J.; Mieremet-Ooms, M. A.; van der Zon, A. M.; van Duijn, W.; van Hogezand, R. A.; Sier, C. F.; Hommes, D. W.; Lamers, C. B.; Verspaget, H. W. *Dig. Liver Dis.* **2007**, *39*, 733.
16. Pyke, C.; Ralfkiær, E.; Huhtala, P.; Ralfkiaer, E.; Hurskainen, T.; Dane, K.; Tryggvason, K. *Cancer Res.* **1992**, *52*, 1336.
17. Chandler, S.; Cossins, J.; Lury, J.; Wells, G. *Biochem. Biophys. Res. Commun.* **1996**, *228*, 421.
18. Dong, Z.; Kumar, R.; Yang, X.; Fidler, I. J. *Cell* **1997**, *88*, 801.
19. Houghton, A. M.; Grisolano, J. L.; Baumann, M. L.; Kobayashi, D. K.; Hautamaki, R. D.; Nehring, L. C.; Cornelius, L. A.; Shapiro, S. D. *Cancer Res.* **2006**, *66*, 6149.
20. Black, R. A.; Rauch, C. T.; Kozlosky, C. J.; Peschon, J. J.; Slack, J. L.; Wolfson, M. F.; Castner, B. J.; Stocking, K. L.; Reddy, P.; Srinivasan, S.; Nelson, N.; Boiani, N.; Schooley, K. A.; Gerhart, M.; Davis, R.; Fitzner, J. N.; Johnson, R. S.; Paxton, R. J.; March, C. J.; Cerreti, D. P. *Nature* **1997**, *385*, 729.
21. Arribas, J.; Esselens, C. *Curr. Pharm. Des.* **2009**, *15*, 2319.
22. Moss, M. L.; White, J. M.; Lambert, M. H.; Andrews, R. C. *Drug Discovery Today* **2001**, *6*, 417.
23. Jones, B. A.; Riegsecker, S.; Rahman, A.; Beamer, M.; Aboualaiwi, W.; Khuder, S. A.; Ahmed, S. *Arthritis Rheum.* **2013**, *65*, 2814.
24. Tursi, A.; Elisei, W.; Principi, M.; Inchingolo, C. D.; Nenna, R.; Picchio, M.; Giorgio, F.; Ierardi, E.; Brandimarte, G. *J Gastrointestin. Liver Dis.* **2014**, *23*, 261.
25. Kirkegaard, T.; Pedersen, G.; Saermark, T.; Brynskov, J. *Clin. Exp. Immunol.* **2004**, *135*, 146.
26. Miller, P. W.; Long, N. J.; Vilar, R.; Gee, A. D. *Angew. Chem., Int. Ed.* **2008**, *47*, 8998.
27. Leeuwenburgh, M. A.; Geurink, P. P.; Klein, T.; Kauffman, H. F.; van der Marel, G. A.; Bischoff, R.; Overkleeft, H. S. *Org. Lett.* **2006**, *8*, 1705.
28. Geurink, P.; Klein, T.; Leeuwenburgh, M.; van der Marel, G.; Kauffman, H.; Bischoff, R.; Overkleeft, H. *Org. Biomol. Chem.* **2008**, *6*, 1244.
29. Whittaker, M.; Floyd, C. D.; Brown, P.; Gearing, A. J. *Chem. Rev.* **1999**, *99*, 2735.
30. Johnström, P.; Clark, J. C.; Pickard, J. D.; Davenport, A. P. *Nucl. Med. Biol.* **2008**, *35*, 725.
31. Wester, H. J.; Hamacher, K.; Stöcklin, G. *Nucl. Med. Biol.* **1996**, *23*, 365.
32. Wüst, F.; Hultsch, C.; Bergmann, R.; Johannsen, B.; Henle, T. *Appl. Radiat. Isot.* **2003**, *59*, 43.
33. Marik, J.; Sutcliffe, J. L. *Appl. Radiat. Isot.* **2007**, *65*, 199.
34. Sounni, N. E.; Devy, L.; Hajitou, A.; Frankenne, F.; Munaut, C.; Gilles, C.; Deroanne, C.; Thompson, E. W.; Foidart, J. M.; Noel, A. *FASEB J.* **2002**, *16*, 555.
35. Köhrmann, A.; Kammerer, U.; Kapp, M.; Dietl, J.; Anacker, J. *BMC Cancer* **2009**, *9*, 188.
36. Bremer, C.; Tung, C. H.; Weissleder, R. *Nat. Med.* **2001**, *7*, 743.
37. Bellac, C. L.; Li, Y.; Lou, Y.; Lange, P. F.; Harwig, C.; Kappelhoff, R.; Dedhar, S.; Adam, M. J.; Ruth, T. J.; Bénard, F.; Perrin, D.; Overall, C. *Cancer Res.* **2010**, *70*, 7562.
38. Temma, T.; Sano, K.; Kuge, Y.; Kamihashi, J.; Takai, N.; Ogawa, Y.; Saji, H. *Biol. Pharm. Bull.* **2009**, *32*, 1272.
39. Shipley, J. M.; Doyle, G. A.; Fliszar, C. J.; Ye, Q. Z.; Johnson, L. L.; Shapiro, S. D.; Welgus, H. G.; Senior, R. M. *J. Biol. Chem.* **1996**, *271*, 4335.
40. Parkar, A. A.; Stow, M. D.; Smith, K.; Panicker, A. K.; Guilloteau, J. P.; Jupp, R.; Crowe, S. J. *Protein Expr. Purif.* **2000**, *20*, 152.